Pain Medicine, 23(2), 2022, 339–346
doi: 10.1093/pm/pnab315
Advance Access Publication Date: 29 October 2021
Brief Report

Neurovascular, Muscle, and Skin Changes on [^{18}F]FDG PET/MRI in Complex Regional Pain Syndrome of the Foot: A Prospective Clinical Study

Daehyun Yoon, PhD,* Yingding Xu, MD,* Peter W. Cipriano, BA,* Israt S. Alam, PhD,* Carina Mari Aparici, MD,* Vivianne L. Tawfik, MD, PhD,† Catherine M. Curtin, MD,‡ Ian R. Carroll, MD,† and Sandip Biswal, MD*

*Departments of Radiology and; †Anesthesiology, Perioperative, and Pain Medicine, Stanford University School of Medicine, Stanford, California, USA; ‡Department of Surgery, Stanford University School of Medicine, Redwood City, California, USA

Correspondence to: Sandip Biswal, MD, Department of Radiology, Stanford University School of Medicine,300 Pasteur Dr., Rm S068B, Stanford, CA 94305, USA. Tel: 1- 650-498-4561; E-mail: biswals@stanford.edu.

The first authorship is shared by two authors, Daehyun Yoon and Yingding Xu, because of equally substantial contributions to study design and analysis.

Funding sources: This study was funded by National Institutes of Health (NIH) P41 EB015891 and General Electric Healthcare.

Conflicts of interest: The authors, Daehyun Yoon, Peter Cipriano, and Sandip Biswal, received research grant support from General Electric Healthcare. Yingding Xu, Israt S. Alam, Carina Mari Aparici, Vivianne L. Tawfik, Catherine M. Curtin, Ian R. Carroll have no potential conflicts to report.

Clinical Trial Information: Registry name: Clinical Trials.gov.

Registration number: NCT03195270.

Registration link: https://clinicaltrials.gov/ct2/show/NCT03195270.

Actual study start date: November 24, 2014.

Received on 25 December 2020; revised on 5 August 2021; Accepted on 1 October 2021

Abstract

Objective. The goal of this study is to demonstrate the feasibility of simultaneous [^{18}F]-fluorodeoxyglucose (FDG) positron emission tomography (PET) and magnetic resonance imaging (MRI) for noninvasive visualization of muscular, neurovascular, and skin changes secondary to complex regional pain syndrome (CRPS). **Subjects.** Seven adult patients with CRPS of the foot and seven healthy adult controls participated in our [^{18}F]FDG PET/MRI study. **Methods.** All participants received whole-body PET/MRI scans 1 hour after the injection of 370MBq [^{18}F]FDG. Resulting PET/MRI images were reviewed by two radiologists. Metabolic and anatomic abnormalities identified, were grouped into muscular, neurovascular, and skin lesions. The [^{18}F]FDG uptake of each lesion was compared with that of corresponding areas in controls using a Mann-Whitney *U*-test. **Results.** On PET images, muscular abnormalities were found in five patients, neurovascular abnormalities in four patients, and skin abnormalities in two patients. However, on MRI images, no muscular abnormalities were detected. Neurovascular abnormalities and skin abnormalities in the affected limb were identified on MRI in one and two patients, respectively. The difference in [^{18}F]FDG uptake between the patients and the controls was significant in muscle ($P = .018$) and neurovascular bundle ($P = .0005$). **Conclusions.** The increased uptake of [^{18}F]FDG in the symptomatic areas likely reflects the increased metabolism due to the inflammatory response causing pain. Therefore, our approach combining metabolic [^{18}F]FDG PET and anatomic MR imaging may offer noninvasive monitoring of the distribution and progression of inflammatory changes associated with CRPS.

Key Words: Complex Regional Pain Syndrome; [^{18}F]FDG PET/MRI; Muscle; Nerve; Skin

© The Author(s) 2021. Published by Oxford University Press on behalf of the American Academy of Pain Medicine.
This is an Open Access article distributed under the terms of the Creative Commons Attribution-NonCommercial License (https://creativecommons.org/licenses/by-nc/4.0/), which permits non-commercial re-use, distribution, and reproduction in any medium, provided the original work is properly cited. For commercial re-use, please contact journals.permissions@oup.com

Introduction

Complex regional pain syndrome (CRPS) is a severe pain condition of extremities, presenting a variety of symptoms that significantly exceeds the expected clinical progression of the injury [1]. Depending on the type of the inciting injury, it is classified into two types: CRPS I if its onset has uncertain history of a causative nerve injury, and CRPS II if it is caused by a confirmed nerve injury. Identical symptoms between both types of CRPS suggest that CRPS type I may be caused by a nerve injury (or injuries) not detectable by currently available clinical methods. Due to the complexity of symptoms and disease progression, it has been very challenging to identify the exact source of pain and design effective treatments for patients with CRPS [2].

A few diagnostic approaches have been adopted to aid the diagnosis of CRPS. Plain film X-ray and three phase bone scan have been used for identifying bone loss or resorption by CRPS. However, these changes may appear temporarily and only at specific stages of CRPS [3, 4]. Magnetic resonance imaging (MRI) facilitated examining pathologic changes in musculoskeletal tissues [5], but its effectiveness has not been fully established yet [3]. Therefore, there is a pressing clinical need for improved localization of the CRPS-induced changes to better understand the disease mechanism and help monitor treatment effects.

In this study, we present preliminary results of a novel imaging approach focusing on the detection of the inflammatory changes due to CRPS. Inflammation without infection is one of the key features of CRPS recognized more than 100 years ago [6]. Positron emission tomography (PET) imaging with [^{18}F]fluorodeoxyglucose (FDG) has been frequently utilized for noninvasive localization of inflamed tissues in many diseases. The low spatial resolution of PET requires paring this technology with another imaging modality that can offer more accurate spatial localization of lesions presenting abnormally high tracer uptake on PET. Typically, PET is coupled with computed tomography (CT) to provide this anatomic map. However, in our study, MRI provides this anatomic guide for PET in the form of a PET/MRI scanner. Of note, MRI is more advantageous than CT due to no extra deposition of ionizing radiation, excellent soft-tissue contrast, and the simultaneous acquisition capability of the recent PET/MRI scanners [7]. We performed a prospective [^{18}F]FDG PET/MRI comparison study on CRPS patients and healthy controls to evaluate its feasibility for noninvasive detection of CRPS-induced changes.

Methods

Human Subjects

Our study has been approved by the institutional review board and all participating subjects signed an informed consent form prior to imaging experiments. Our study protocol follows guidelines for human experiments by the Declaration of Helsinki [8]. All research data such as participant information and images were acquired in compliance with the Health Insurance Portability and Accountability Act. The clinical trial registration number of this study is NCT03195270 (https://clinicaltrials.gov/ct2/show/NCT03195270).

Seven patients who were diagnosed with CRPS of the foot on the basis of symptoms and signs concordant with the Budapest criteria [9] were enrolled in our study. The diagnosis was made by pain physicians (V.T., I.C.) and plastic surgeon (C.M.) at the clinical sites of our institution. The initial evaluation results of the patients, including the pain location, duration, CRPS type, pain ratings, and previous treatments, are summarized in Table 1. Except for Patient 3, all patients had unilateral pain. It should be noted that all patients had received standard-of-care diagnostic exams and treatments prior to our study and failed to have a satisfactory outcome. All patients were female, and the mean ± standard deviation/range of their age was 38.7 ± 12.4 years/20–54 years. Seven healthy controls were recruited to compare the [^{18}F]FDG uptake (four males and three females; 30.2 ± 1.1 years/29–32 years for males, 29.7 ± 6.1 years/22–37 years for females).

PET/MR Imaging Procedure

Pre-imaging preparation: Subjects were prohibited from any physical exercise for 24 hours prior to imaging to suppress the unrelated metabolic activities. The blood glucose level of subjects was maintained under 10 mmol/L by fasting for at least four hours prior to the imaging session. The use of anxiolytics was permitted, if necessary, to help subjects remain settled during the scan. A single 370MBq dose of [^{18}F]FDG was administered intravenously to the subject one hour before imaging. Then, the subject was seated to take a rest and avoid muscle activities until the admission to the PET/MRI scanner.

PET/MRI imaging: Simultaneous PET and MRI scans covering the whole body in eight to ten stations were performed depending on the height of the patient in a GE PET/MRI scanner (SIGNA PET/MR, General Electric Healthcare, Waukesha, Wisconsin, USA). Two anterior body array coils were placed on the subject for MRI signal reception and immobilization of the subject. At each station, a fast T1-weighted scan with two-point Dixon was acquired to conduct attenuation correction for PET images. A T2-weighted scan with fat suppression was conducted for those stations covering the symptomatic areas.

PET image reconstruction: The derivation of attenuation coefficient maps from the MRI images and attenuation correction for the PET image reconstruction were automatically handled during the scan by the algorithm offered by the vendor of the scanner [10, 11]. The ordered subsets expectation maximization algorithm [12] implemented by the vendor was used to reconstruct the PET images. The in-plane resolution of resulting PET images was 3.1 mm × 3.1 mm and the slice thickness was

Table 1. Initial evaluation results of the recruited CRPS patients

Patient Number	Pain Symptom Location	Pain Ratings	Duration	CRPS Type	Previous Ineffective Treatments
1	Right foot/leg	8 to 9 out of 10	7 years	I	Lipomatous mass resection, Nerve pain medications
2	Left foot/ankle	5 to 9 out of 10	5 years	I	Opioid medications, Nerve pain medications, Lumbar sympathetic block, Steroid injections
3	Bilateral foot/leg	7 to 10 out of 10	5 years	I	Nerve pain medications, Pamidronate infusion, Lumbar sympathetic block, Sciatic & saphenous nerve block, Plantar nerve release.
4	Right foot	5 out of 10	4 years	I	Ketamine infusion, Opioid medications, Nerve pain medications, Lumbar sympathetic blocks, Transcutaneous electrical nerve stimulation
5	Right foot/leg	10 out of 10	2 years	I	Multiple popliteal nerve blocks, Spinal cord stimulation
6	Left foot/leg	4 to 6 out of 10	2 years	II	Saphenous nerve block, Ketamine infusion, Transcutaneous electrical nerve stimulation, Lumbar sympathetic plexus block
7	Left foot	5 to 10 out of 10	7 years	I	Multiple saphenous nerve blocks, Ultrasound-guided radiofrequency ablation of the saphenous nerve

Pain ratings were on a 0 to 10 scale where 0 is no pain and 10 is the worst pain. CRPS = complex regional pain syndrome.

2.8 mm. An in plane Gaussian filter with 3.5 mm full-width at half maximum was applied for smoothing.

Image Review

A radiologic review of [^{18}F]FDG PET and MRI images were independently performed by two board-certified radiologists. For the review of PET images, attenuation-corrected PET images in the unit of standardized uptake value (SUV) were used. Lesions with focally increased [^{18}F]FDG uptake of the symptomatic areas were identified by comparison with the [^{18}F]FDG uptake of the local background and corresponding areas of healthy controls. MRI images were reviewed to identify lesions presenting either abnormally increased signal on the T2-weighted contrast or showing abnormal structural changes. Horos software (https://horosproject.org/) was used for the display and analysis of PET and MRI images.

Statistical Analysis

Abnormalities detected on PET and MRI were classified into three tissue categories: muscle, neurovascular bundle, and skin/subcutaneous tissue. Note that the further classification of tissue types, such as peripheral nerves, blood vessels, and skins, was not feasible due to the limited spatial resolution of PET. For each lesion on the PET images, a circular region of interest (ROI) fitting the lesion was manually drawn to measure the maximum standardized uptake value (SUV_{max}). For each control, the SUV_{max} of each tissue type in the foot and lower extremities was measured. Then, for each tissue type, the group of SUV_{max} from associated lesions from patients was compared with the group of SUV_{max} from healthy controls. The sample size of seven provides 80% power to detect a difference as small as 1.5 standard deviation with two-sided 5% error. Mann-Whitney *U*-test was employed for comparison with the *P* values of .05 adopted as a significance level. The mean and the standard deviation of SUV_{max} of the patients and the healthy controls was also calculated for individual tissue groups.

Results

PET/MRI Image Review

Abnormalities were found at the reported site of pain in all seven patients on [^{18}F]FDG PET, but in only three patients on MRI (Table 2). Increased uptake on foot muscles was the most frequent finding on PET (five patients), while, on MRI, skin thickening, and nerve abnormalities were the most frequent observation (two patients, respectively). Figure 1 shows focally increased [^{18}F]FDG uptake on the left extensor digitorum brevis muscle (Figure 1A, 1D) from a patient with left dorsal foot pain and on the left flexor digitorum brevis muscle (Figure 1B, 1E) from a patient with left plantar foot

Table 2. Identified [18F]FDG PET and MRI abnormalities of foot muscles, neurovascular bundles, and skin from seven CRPS patient participants

Patient Number	Modality	Muscle	Neurovascular Bundle	Skin
1	PET	High FDG uptake on right dorsal foot muscles	None	None
	MRI	None	None	None
2	PET	High FDG uptake on left plantar foot muscles	None	None
	MRI	None	None	None
3	PET	High FDG uptake on left plantar foot muscles	High FDG uptake on bilateral plantar, tibial, femoral, popliteal nerves	None
	MRI	None	None	None
4	PET	High FDG uptake on right ankle scar, muscles	High FDG uptake on right posterior tibial nerve	None
	MRI	None	None	None
5	PET	None	None	High FDG uptake on subcutaneous/skin tissue from the right distal thigh to the foot
	MRI	None	None	Skin thickening and subcutaneous edema throughout the right leg
6	PET	None	High FDG uptake on left saphenous nerve	High FDG uptake on subcutaneous tissue around left medial and lateral malleoli
	MRI	None	Enlarged left saphenous nerve	Subcutaneous tissue thickening around left medial and lateral malleoli
7	PET	High FDG uptake on left dorsal foot muscles	High FDG uptake on the left saphenous nerve	None
	MRI	None	Increased signal on the left saphenous, sural nerves	None

CRPS = complex regional pain syndrome; FDG = [^{18}F]-fluorodeoxyglucose; MRI = magnetic resonance imaging; PET = positron emission tomography.

pain. Images from a healthy control (Figure 1C, 1F) show a representative example of [^{18}F]FDG PET/MRI images with no abnormalities. Locally and globally increased [^{18}F]FDG uptake on neurovascular bundles are respectively presented in Figures 2 and 3. The right tibial neurovascular bundle passing through the scar tissue at the ankle showed high [^{18}F]FDG uptake from a patient with right foot pain (Figure 2A, 2B), which become more obvious when compared to images from a healthy control (Figure 2B, 2D). Figure 3 compares [^{18}F]FDG PET images from a representative control (3A) and a patient with bilateral foot and leg pain presenting significantly high [^{18}F]FDG uptake bilaterally on femoral, popliteal, and tibial neurovascular bundles (Figure 3B). Figure 4 displays a case of skin and subcutaneous tissue abnormalities on both [^{18}F]FDG PET (Figure 4A) and coregistered PET/MRI (4C) images from a patient with right foot and lower leg pain. Compared to the images from a similar slice location of a healthy control (Figure 4B, 4D), the patient images present multiple sites of focally increased [^{18}F]FDG uptake with skin edema and thickened subcutaneous tissue.

[^{18}F]FDG Uptake Comparison

Detected lesions of CRPS patients showed significantly higher [^{18}F]FDG uptake than the corresponding regions in healthy controls (Figure 5). The mean ± standard deviation of SUV_{max} between the detected lesions from CRPS patients and corresponding tissues from healthy controls were 1.29 ± 0.29 vs 0.86 ± 0.19 (muscle), 1.38 ± 0.57 vs 0.73 ± 0.10 (neurovascular bundle), and 3.10 ± 2.97 vs 0.44 ± 0.08 (skin/subcutaneous tissues). The mean ± standard deviation of SUV_{max} between the healthy male controls and female controls were 0.85 ± 0.09/0.87 ± 0.25 (muscle), 0.78 ± 0.04/0.67 ± 0.09 (neurovascular bundle), and 0.48 ± 0.04/0.4 ± 0.08 (skin/subcutaneous tissues). The P values from the SUV_{max} comparison in muscular and neurovascular tissues were .018 and .0005, respectively, indicating a significant difference between patients and healthy controls. The P values for the skin/subcutaneous tissue comparison could not be computed due to a limited sample size.

Discussion

In this study, we evaluated the feasibility of [^{18}F]FDG PET/MRI to detect metabolic and anatomic changes associated with CRPS. Radiologic evaluation and quantitative comparison confirmed that all seven patients with CRPS of the foot exhibited significantly increased metabolism on [^{18}F]FDG PET ($P < .05$), possibly from inflammatory processes in CRPS. However, the [^{18}F]FDG

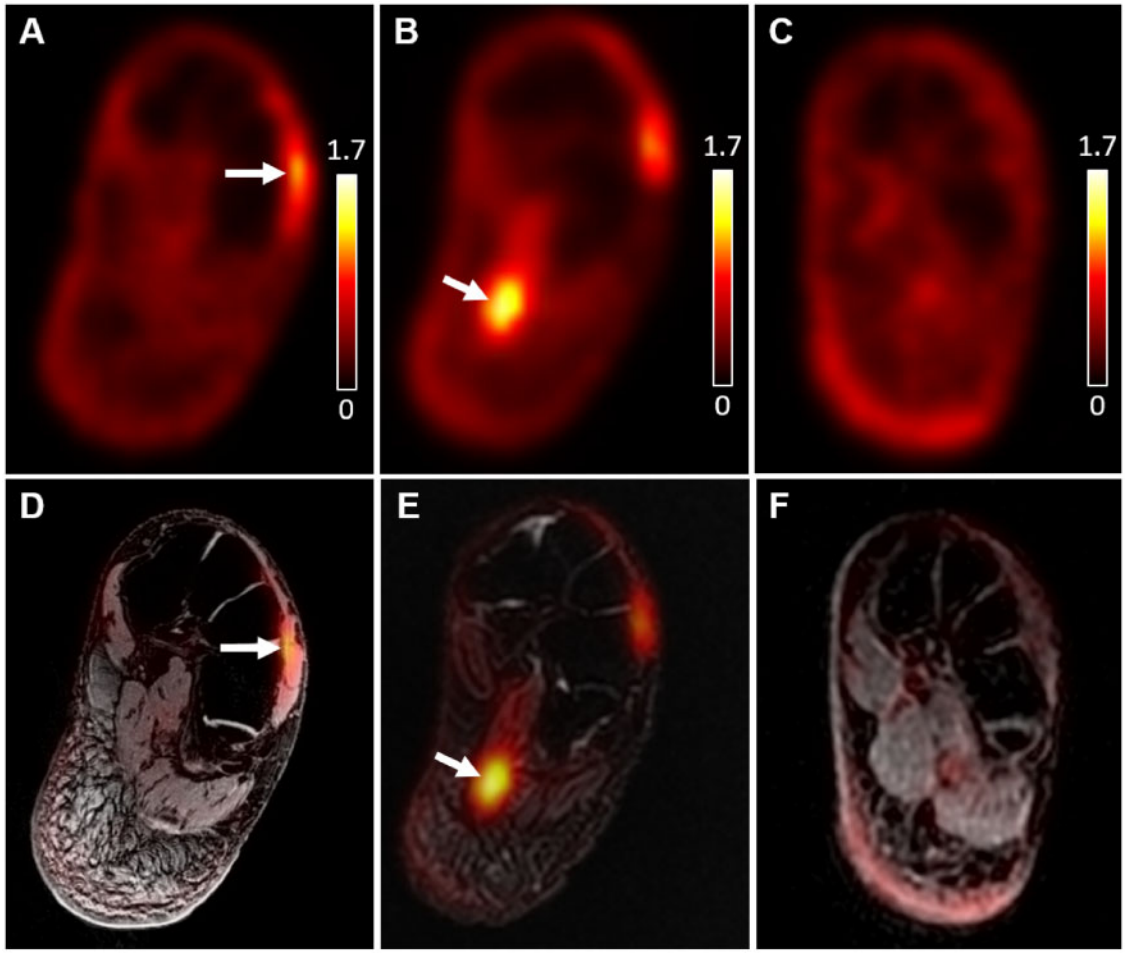

Figure 1. Locally high [^{18}F]FDG uptake on foot muscles at the site of pain symptom from two patients in comparison with no abnormalities of a healthy control subject. High [^{18}F]FDG uptake was identified (red arrows) on the left extensor digitorum brevis muscle (**A:** PET only, **D:** PET/MRI coregistered) from Patient 7 and left flexor digitorum brevis muscle (**B:** PET only, **E:** PET/MRI coregistered) from Patient 2. No structural damage or abnormal signal intensity was observed on the MRI image. The PET-only image (**C**) and PET/MRI coregistered image (**F**) at a similar slice location from a control subject do not show focally increased [^{18}F]FDG uptake or structural abnormalities. The unit of PET signal on the images is SUV. The same color scale (0–1.7) was used for all subfigures for PET. MRI = magnetic resonance imaging; PET = positron emission tomography.

uptake values of identified lesions and their difference from control uptake values were relatively small compared to those reported in [^{18}F]FDG PET studies of more common target diseases, such as cancer. This may suggest that a different standard or threshold should be applied to identify the abnormalities in the [^{18}F]FDG PET images of CRPS. Also, no single common abnormality was found in the affected limbs across all patients, reflecting the complicated heterogeneity of CRPS pathology.

Gross morphologic changes or signal abnormalities on MRI were identified at the site of elevated [^{18}F]FDG uptake, but only from three of the seven patients studied (Patients 5, 6, and 7). This suggests metabolic interrogation with [^{18}F]FDG PET may identify CRPS-induced changes earlier than MRI, and therefore potentially promote early and effective management of CRPS [13]. However, this improved sensitivity of [^{18}F]FDG PET to potential changes by CRPS could not remove the need for the combination with MRI. This is because the tissue classification of lesions with high [^{18}F]FDG uptake was only enabled by structural MRI data. For example, the subcutaneous tissue uptake in Figure 4 would probably have been misclassified into the muscle uptake if judged only by its location on PET images.

Our imaging findings may facilitate specific subtyping or staging of CRPS. All abnormal PET uptake was locally confined except the case of Patient 3 presenting the global uptake on multiple neurovascular bundles (Figure 3B). This likely supports the reported heterogeneity in the disease mechanism of CRPS [14], which could impart differing management approaches. High [^{18}F]FDG uptake on the edematous skin and subcutaneous tissue (Figure 4) is another feature that could be unique to a specific subtype or stage of CRPS. Hypermetabolic edema as shown in Figure 4 may also

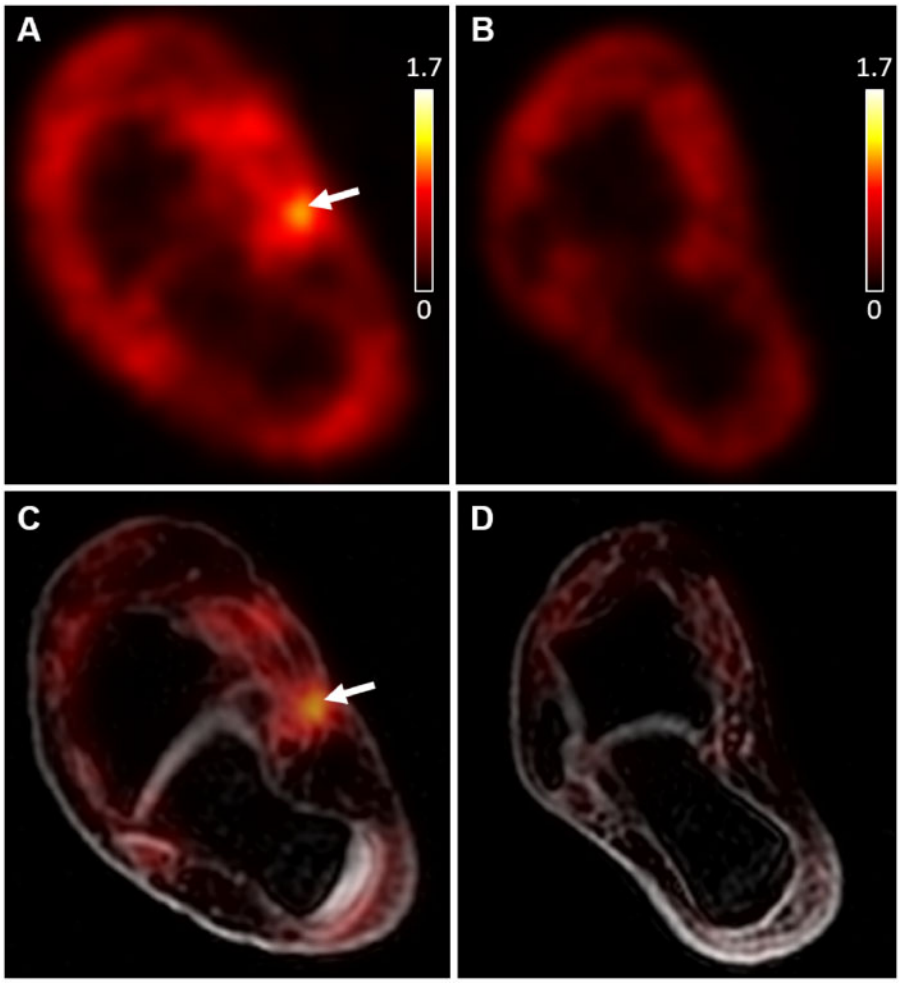

Figure 2. Increased [^{18}F]FDG uptake on neurovascular bundles at the site of pain symptom from a patient in comparison with no abnormalities from a healthy control. Locally increased [^{18}F]FDG uptake was detected on the tibial neurovascular bundle passing through the scar tissue at the ankle of Patient 4 and marked by the yellow arrow (**A**: PET only, **C**: PET/MRI coregistered). Again, the PET-only image (**B**) and PET/MRI coregistered image (**D**) at a similar slice location from a healthy control subject shows no abnormalities. The unit of PET signal on the images is SUV. The same color scale (0–1.7) was used for all subfigures for PET. MRI = magnetic resonance imaging; PET = positron emission tomography.

indicate a possibility to identify an inflammatory subtype of CRPS because edema is supposedly composed of body fluid, lacking the cellular components for increased metabolism. However, this may need further validation because the elevated uptake of [^{18}F]FDG can be also related to extravasated blood pool or increased volume of inflammation/infection. It should be also noted that three cases of CRPS type I showed abnormal [^{18}F]FDG uptake on peripheral nerves, while the only case of CRPS type II presented both PET and MRI abnormalities at the suspected nerve. This suggests that our method may provide the increased sensitivity to the causative nerve damage for the improved distinction between CRPS type I and II.

Our study has a few limitations. First, the number of enrolled patients and healthy controls was insufficient to conduct an age-sex matched comparison or group our heterogenous findings and associate them with specific aspects of CRPS. Our validation of the detected abnormalities regarding their potential contribution to pain is supported by their location, radiologic review and statistical comparison. However, a more direct evaluation of their association with pain, such as the outcome assessment of local anesthetic injection to detected abnormalities, would be desirable. Rescanning of the patient after treatments to associate the change of the abnormal uptake with the pain assessment could be another option. There may be a chance that factors other than inflammation, such as increased muscle recruitment from limping, could result in increased muscular uptake of [^{18}F]FDG in the favored limb. It is also possible that the asymptomatic contralateral limb may have nonspecific increase of [^{18}F]FDG uptake due to limping, compensatory movements, and overuse. Therefore, additional diagnostic information, potentially through developments of novel MRI techniques in our case, might be necessary to improve the specificity.

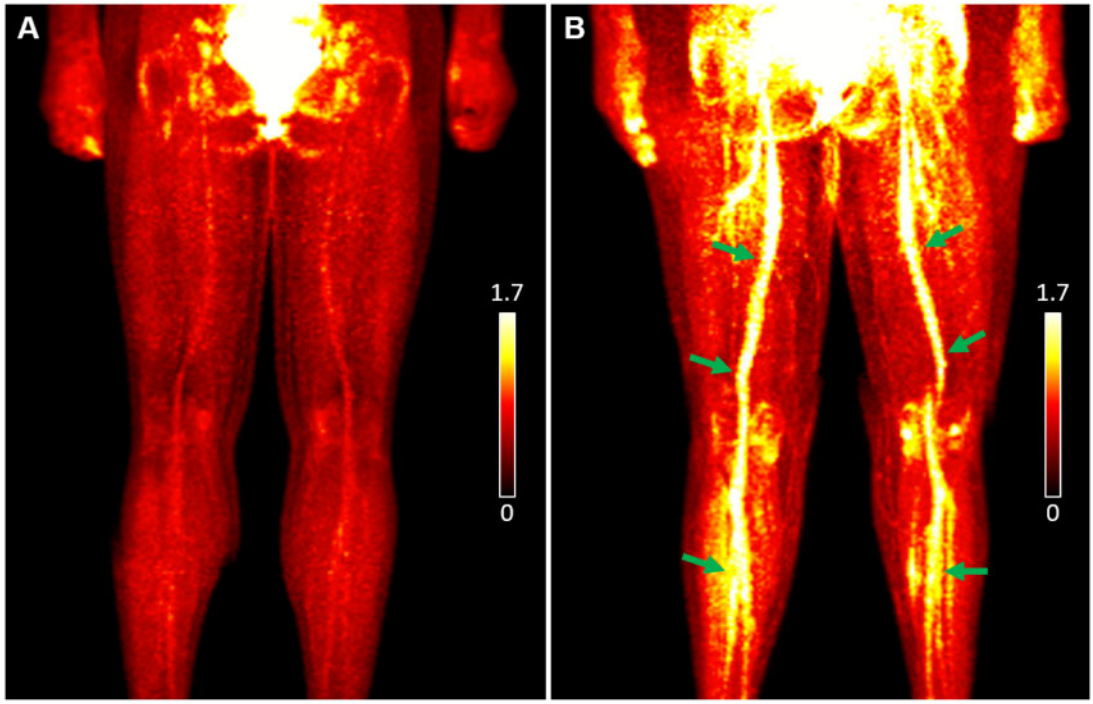

Figure 3. Globally Increased [^{18}F]FDG uptake on neurovascular bundles along the site of pain symptom on maximum intensity projection PET images. Healthy controls did not present noticeably high [^{18}F]FDG uptake on neurovascular bundles compared to the background tissues as shown in a representative control (**A**: PET only). However, a significantly increased [^{18}F]FDG uptake was found bilaterally on multiple neurovascular bundles from Patient 3 with bilateral foot and leg pain (**B**: PET only, white arrows). The unit of PET signal on the images is SUV. The same color scale (0–1.7) was used for all subfigures. MRI = magnetic resonance imaging; PET = positron emission tomography.

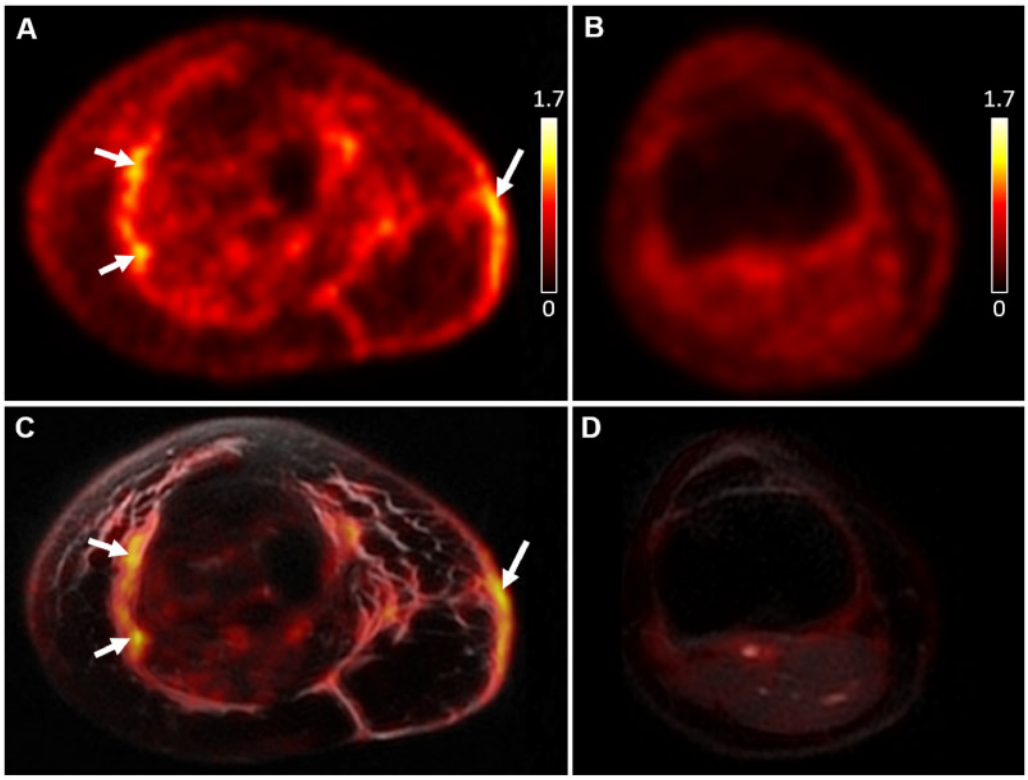

Figure 4. [^{18}F]FDG PET and MRI abnormalities of skin and subcutaneous tissue of the symptomatic lower leg from Patient 5 (**A**: PET only, **C**: PET/MRI coregistered) in comparison with no abnormalities on the PET-only image (**B**) and PET/MRI coregistered image (**D**) from a healthy control subject. Increased uptake of [^{18}F]FDG was identified on PET (white arrows) where edematous skin and subcutaneous tissue thickening was detected on MRI. The unit of PET signal on the images is SUV. The same color scale (0–1.7) was used for all subfigures for PET. MRI = magnetic resonance imaging; PET = positron emission tomography.

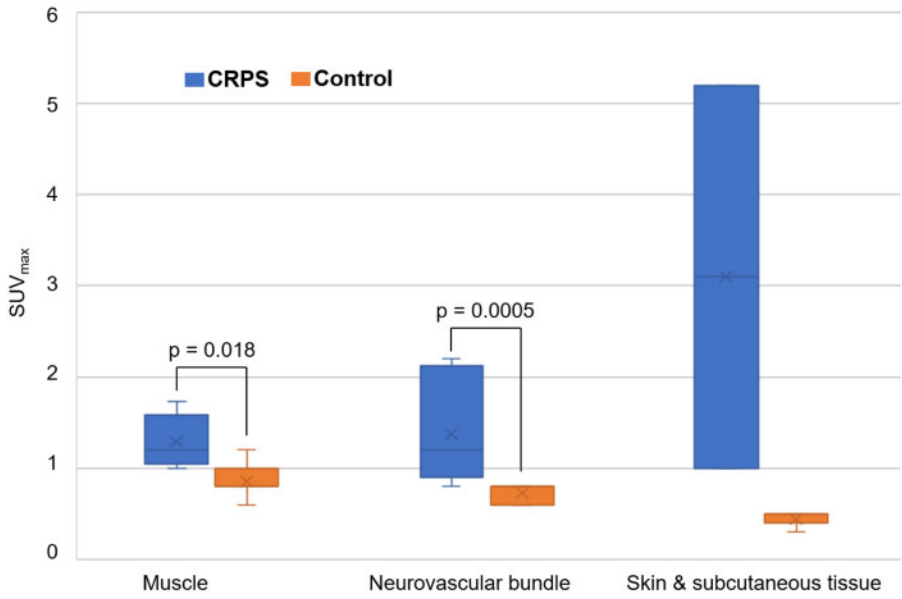

Figure 5. Mean and standard deviation of [^{18}F]FDG SUV_{max} in muscle, neurovascular bundle, and skin lesions of CRPS patients and corresponding tissues of healthy controls. SUV_{max} in the lesions in muscle and nerve tissues show statistically significant differences than controls ($P < .05$). CRPS = complex regional pain syndrome.

Conclusion

We present a novel [^{18}F]FDG PET/MRI approach that identified metabolic and structural abnormalities in muscles, neurovascular bundles, and skin likely due to the inflammatory process of CRPS. Our preliminary results demonstrate the diagnostic potential of this approach for the noninvasive monitoring of distribution and progression of CRPS-induced changes.

Acknowledgments

This study was supported by NIH P41 EB015891 and General Electric Healthcare.

References

1. Janig W, Baron R. Complex regional pain syndrome: Mystery explained? Lancet Neurol 2003;2(11):687–97.
2. Birklein F, Handwerker HO. Complex regional pain syndrome: How to resolve the complexity? Pain 2001;94(1):1–6.
3. Schurmann M, Zaspel J, Lohr P, et al. Imaging in early posttraumatic complex regional pain syndrome: A comparison of diagnostic methods. Clin J Pain 2007;23(5):449–57.
4. Lee GW, Weeks PM. The role of bone scintigraphy in diagnosing reflex sympathetic dystrophy. J Hand Surg Am 1995;20(3):458–63.
5. Graif M, Schweitzer ME, Marks B, Matteucci T, Mandel S. Synovial effusion in reflex sympathetic dystrophy: An additional sign for diagnosis and staging. Skeletal Radiol 1998;27(5):262–5.
6. Iolascon G, de Sire A, Moretti A, Gimigliano F. Complex regional pain syndrome (CRPS) type I: Historical perspective and critical issues. Clin Cases Miner Bone Metab 2015;12(Suppl 1):4–10.
7. Cipriano PW, Yoon D, Gandhi H, et al. (18)F-FDG PET/MRI in chronic sciatica: Early results revealing spinal and nonspinal abnormalities. J Nucl Med 2018;59(6):967–72.
8. World Medical Association. World Medical Association Declaration of Helsinki: Ethical principles for medical research involving human subjects. JAMA 2013;310(20):2191–4.
9. Harden RN, Bruehl S, Perez RS, et al. Validation of proposed diagnostic criteria (the "Budapest Criteria") for Complex Regional Pain Syndrome. Pain 2010;150(2):268–74.
10. Sekine T, Buck A, Delso G, et al. Evaluation of atlas-based attenuation correction for integrated PET/MR in human brain: Application of a head atlas and comparison to true CT-based attenuation correction. J Nucl Med 2016;57(2):215–20.
11. Wollenweber SD, Ambwani S, Lonn AHR, et al. Comparison of 4-class and continuous fat/water methods for whole-body, MR-based PET attenuation correction. IEEE Trans Nucl Sci 2013;60 (5):3391–0.
12. Hudson HM, Larkin RS. Accelerated image reconstruction using ordered subsets of projection data. IEEE Trans Med Imaging 1994;13(4):601–9.
13. Kingery WS. A critical review of controlled clinical trials for peripheral neuropathic pain and complex regional pain syndromes. Pain 1997;73(2):123–39.
14. David Clark J, Tawfik VL, Tajerian M, Kingery WS. Autoinflammatory and autoimmune contributions to complex regional pain syndrome. Mol Pain 2018;14:1744806918799127.